Journal of Applied Electrochemistry (2005) 35:539–544
DOI 10.1007/s10800-005-1517-y

Internal stress in multilayer silver–bismuth coatings

I. KRASTEV[1,*], T. VALKOVA[1] and A. ZIELONKA[2]
[1]*Institute of Physical Chemistry, Bulgarian Academy of Sciences, 1113 Sofia, Bulgaria*
[2]*Forschungsinstitut für Edelmetalle und Metallchemie, 73525 Schwäbisch Gmünd, Germany*
*(*author for correspondence, e-mail: krastev@ipchp.ipc.bas.bg)*

Received 18 August 2004; accepted in revised form 15 January 2005

Key words: electrodeposition, internal stress, multilayer, silver–bismuth alloys, structure

Abstract

An investigation was carried out on the influence of electrodeposition conditions on internal stress of cyclically modulated Ag–Bi alloys. Pulse currents of different duration and height were used, leading to different composition and thickness of the deposited sublayers, and the resulting changes in the internal stress were measured *in situ*. The investigated multilayer coatings with Bi contents up to 20 wt.% reveal a positive (tensile) internal stress, and at Bi contents higher than 20 wt.% the internal stress is negative (compressive). The possibility of deposition of stress-free coatings is shown.

1. Introduction

In an effort to reduce some of the disadvantages of electrodeposited silver coatings, e.g. poor hardness and wear resistance, susceptibility to tarnishing and relatively high friction coefficient, silver is alloyed with different metals. In most of the cases alloys containing small amounts of the alloying element are used, leading to improvement in the mechanical parameters of the coating, mainly when solid solutions and intermetallic compounds of silver with the respective metals are formed. In the latter case internal stress in the electrodeposited coating originating from the differences in the size of various metal atoms may result in an increase in hardness and wear resistance in coatings [1]. Similar conclusions have been derived during the investigation of the Ag–Sb system [2, 3].

The Ag–Bi alloy is used in the field of electronics, communication equipment production and for coating subjected to operation under hard conditions [4, 5]. The alloy is deposited mainly in alkaline electrolytes. In previous work we have studied the electrochemical relationships during the electrodeposition of silver [6], bismuth [7] and Ag–Bi alloy [8, 9].

According to the phase diagram bismuth displays a very low solubility (up to 3 wt.%) in solid-state silver [10]. The maximum solubility of bismuth in silver in the electrodeposited alloy reaches approximately 2.5 wt.% [11] and higher concentrations should lead to the appearance of a second phase in the electroplated coating.

In many cases when investigating cross-section cuts of alloy coatings (e.g. Ag–Sb, Ag–Pb, etc.) it is established that they display a lamellar, layered structure. In similar cases the coatings are composed of darker and lighter lamellas containing larger or smaller amounts of the alloying element. The Ag–Bi alloy coatings are heterogeneous, two-phase and are composed of regions containing almost pure silver or pure bismuth [12]. The spatial separation of the two phases leads to the formation of a columnar structure, onto which in some cases a superpositioned lamellar structure is observed. Some of the properties of the alloy coatings electrodeposited under various conditions are described in a previous paper [12]. For example, when the percentage of bismuth in the coating increases, negative internal stress is produced as a result of both the stretching of the silver lattice at low bismuth concentration and the formation of a solid phase solution, as well as the stress of the pure bismuth phase of the heterogeneous alloy coatings [12]. The formulation of the electrolyte is optimised in such a way that offers a possibility to electrodeposit Ag–Bi alloy coatings with random percentage composition; i.e. coatings containing bismuth within the range 0–100% may be plated [9].

The present paper is aimed at the electrodeposition of multilayer cyclically modulated Ag–Bi alloy coatings and investigation of the internal stress as a function of the composition and thickness of the separate sublayers.

2. Experimental

The composition of the electrolyte is presented in Table 1. The method for the preparation of the electrolyte is described in a previous paper [9].

Table 1. Electrolyte composition

Components	Concentration /g dm^{-3}	Concentration /mol dm^{-3}
Ag as $KAg(CN)_2$	8	0.074
Bi as $BiONO_3$	18	0.086
NaOH	26	0.64
$KNaC_4H_4O_6{\cdot}4H_2O$	60	0.213

The multilayer coatings were electrodeposited in a single bath by galvanostatically changing the current between two different levels, corresponding to the electrodeposition of alloys with higher or lower bismuth content. The current pulses were applied using a programmable pulse generator Pragmatic Instruments 2411A through a bipolar operational amplifier (Kepco, BOP 20–10 M).

The internal stress of the coatings was measured with the Stalzer instrument [13] based on the bent cathode method. The experimental equipment and the equation for calculating internal stress are described in a previous paper [14]. The signal obtained by the sensor of the instrument is connected via a suitable interface to a PC for further processing and storage. The figures concerning internal stress in the present paper show this signal, which provides more information than the stress value itself [3].

In some cases, parallel to these measurements the potential of the working electrode resulting from the applied current pulses was determined. Registration of the alterations of the potential was carried out with a potentiostat–galvanostat model M270 made by the PAR Company using a SCE reference electrode. The latter was fixed in a separate cell containing 3 M KCl aqueous solution and the connection with the Haber–Luggin capillary in the electrodeposition and stress measurement cell was by a 3 M KCl filled electrolytic bridge. The working electrodes were copper plates $10.5 \times 1 \times 0.03$ cm onto which the alloy coating was electrodeposited on the front face upon an area of 7×1 cm. The rear face of the plate was insulated with a suitable varnish.

The composition and thickness of the electrodeposited coatings were determined by X-ray fluorescent analysis with a Fischerscope XDVM-WW instrument. Pure silver anodes were used. All experiments were carried out at room temperature.

3. Results

Figures 1 and 2 show the changes of the sensor signal related to the internal stress during the electrodeposition of both monolayer and multilayer coatings. The individual sublayers of the multilayer coatings were plated at current densities identical to the values used for the electrodeposition of the corresponding monolayer coatings.

The internal stress of the coatings electrodeposited at 0.2 A dm^{-2} have low positive values, typical for pure silver plates deposited using similar electrolytes [3, 15].

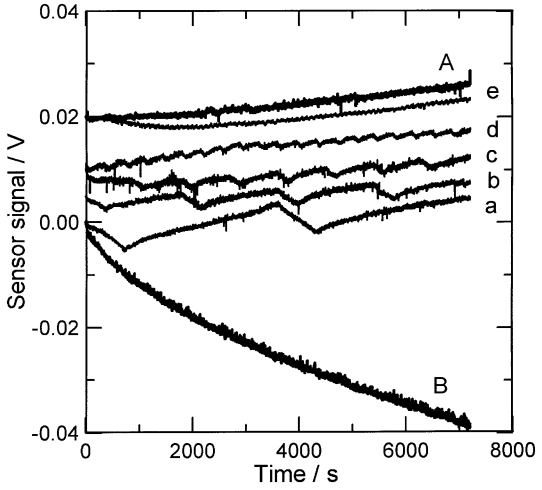

Fig. 1. Change of the sensor signal with time $C_{Ag} = 8$ g dm^{-3}, $C_{Bi} = 18$ g dm^{-3}; $J_1{:}J_2 = 0.8{:}0.2$ A dm^{-2}; $t_1{:}t_2 = 1{:}4$ (A) monolayer, 0.2 A dm^{-2}, 0.7 wt.% Bi, 12.5 μm, $(U-U_o)$ + 0.02 V (B) monolayer, 0.8 A dm^{-2}, 50 wt.% Bi, 26.3 μm (a) 4 sublayer, 14.0 wt.% Bi, 18.1 μm, $(U-U_o)$ + 0.005 V (b) 8 sublayer, 18.3 wt.% Bi, 18.2 μm, $(U-U_o)$ + 0.01 V (c) 16 sublayer, 20.2 wt.% Bi, 18.9 μm, $(U-U_o)$ + 0.01 V (d) 40 sublayer, 22.2 wt.% Bi, 18.3 μm, $(U-U_o)$ + 0.01 V (e) 160 sublayer, 26.2 wt.% Bi, 18.5 μm, $(U-U_o)$ + 0.02 V.

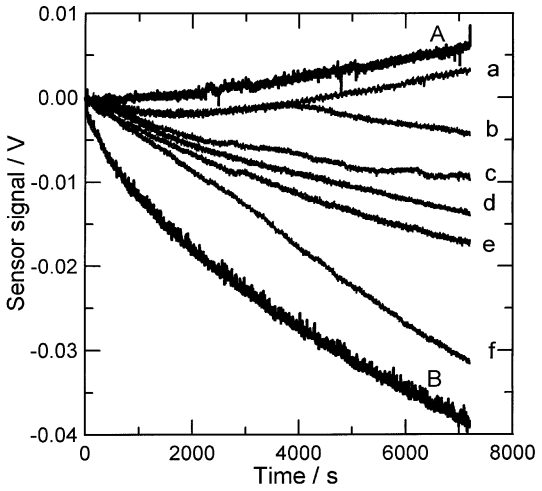

Fig. 2. Change of the sensor signal with time $C_{Ag} = 8$ g dm^{-3}, $C_{Bi} = 18$ g dm^{-3}; $J_1{:}J_2 = 0.8{:}0.2$ A dm^{-2}; $t_1{:}t_2 = 1{:}4$ (A) monolayer, 0.2 A dm^{-2}, 0.7 wt.% Bi, 12.5 μm (B) monolayer, 0.8 A dm^{-2}, 50 wt.% Bi, 26.3 μm (a) 160 sublayer, 26.2 wt.% Bi, 18.5 μm (b) 400 sublayer, 28.2 wt.% Bi, 20.4 μm (c) 800 sublayer, 26.4 wt.% Bi, 18.9 μm (d) 8000 sublayer, 24.5 wt.% Bi, 19.0 μm (e) 16000 sublayer, 25.8 wt.% Bi, 20.6 μm (f) 40000 sublayer, 33.4 wt.% Bi, 22.0 μm.

At higher current densities (0.8 A dm^{-2}) negative internal stress is registered, also in accordance with relationships established during other investigations [12]. When multilayer coatings 18 μm thick are deposited at the stated current densities ($J_1{:}J_2 = 0.8{:}0.2$ A dm^{-2}; $t_1{:}t_2 = 1{:}4$) characteristic regions on the curves showing the changes of the sensor signal vs. time are registered, corresponding to the internal stress in the coating electrodeposited at one of the two current densities (Figure 1). The internal stress of this multilayer system at

relatively substantial thickness of the individual sublayers, respectively small number of sublayers is situated completely in the positive region, although some sectors of the curves correspond to negative stress originated by the contribution of the high current density. As the thickness of the sublayers is reduced to approximately 0.5 μm (40 sublayers – curve d), the effect of individual sublayers upon changes in internal stress is evident. The effect can not be registered during further reduction of sublayer thickness and the curve acquires a linear shape.

The internal stress of coatings deposited under identical conditions (J_1:J_2 = 0.8:0.2 A dm^{-2}; t_1:t_2 = 1:4) theoretically corresponding to 400–40,000 sublayers is presented in Figure 2.

A substantial reduction in sublayer thickness leads to a transition from overall positive to overall negative internal stress in the coating. The latter increases as the number of sublayers increases. Meanwhile an increase in bismuth content in the coatings is established (compare with Figure 4), which is probably the reason for the increase in internal stress in the negative direction. This relationship confirms the conclusion reached in other investigations that the negative internal stress in the system is due not only to the stretching of the silver crystal lattice (alpha phase) by the codeposited bismuth atoms, but also to the simultaneous electrodeposition of the pure bismuth phase, which should also display negative stress [12]. It is well known that bismuth is a metal which increases in volume during solidification and internal stress originating during this process should be negative [5].

In addition, the percentage content of bismuth in the deposited coatings is considerably in excess of 2.5 wt.% – the amount required for the saturation of the silver lattice according to the phase diagram. During the shortest current pulses the internal stress of the system is most strongly affected by the high current density and reaches values characteristic for monolayer alloy coatings electrodeposited at 0.8 A dm^{-2}.

The change in cathodic potential with time when depositing multilayer coatings with equal thickness of the two types of sublayers is presented in Figure 3. The shift from low to high current density is accompanied by an abrupt change in potential and relatively rapid establishment of a new steady-state value during sufficiently long pulses (Figure 3a). As the length of the pulses decreases, i.e. the number of sublayers increases (Figure 3b, c) the high current density is not abruptly established, but rather gradually. The reverse shift from high to low current density is always related to the gradual smooth change of potential and relatively slow establishment of its steady state value.

Figure 4 shows that the bismuth content in the coating increases both during longer electrodeposition of the richer in bismuth content sublayer at higher current density as well as when the number of sublayers is increased. It may be possible that the difference in the susceptibility to deposition of the two metals one over the other also contributes to this effect.

When retaining the same ratio of current densities, corresponding to the identical composition of the alloy in the individual layers, but changing the ratio of deposition times (t_1:t_2 = 1:9), multilayer coatings with reduced thickness of the bismuth-rich sublayer and increased thickness of the silver-rich sublayer are obtained respectively. The thickness of the individual sublayers in this case is in the ratio 1:2.25 in favour of the silver-rich sublayer.

Figures 5 and 6 show the internal stress of the coatings deposited at the mentioned ratio of the thickness of both types of sublayer. In the case of very thick sublayers the overall internal stress of the multilayer coatings is affected by the contribution of the much thicker and silver-rich sublayer and has a positive sign (Figure 5). The overall percentage of bismuth in the coatings is low (10–18 wt.%).

As the number of sublayers is increased, internal tensile stress initially increases (Figure 6), followed by a relaxation of the system at increased pulse frequency and almost strain-free coatings are deposited (Figures 6c, d, e) in the case of the thinnest sublayers.

The relationships presented in Figures 1–6 may lead to the conclusion that at bismuth content approximately up to 20 wt.% positive internal stress is registered in the electrodeposited multilayer coatings.

The overall percentage content of bismuth in the coating can be increased by increasing the thickness of the bismuth-richer sublayer, i.e. by changing the ratio of deposition times (e.g. t_1:t_2 = 2:3). In this case the increase is from 22 to 44 wt.% as the number of sublayers is increased. The internal stress of similar coatings is shown in Figures 7 and 8. Within the entire range of sublayer thickness compressive internal stress is

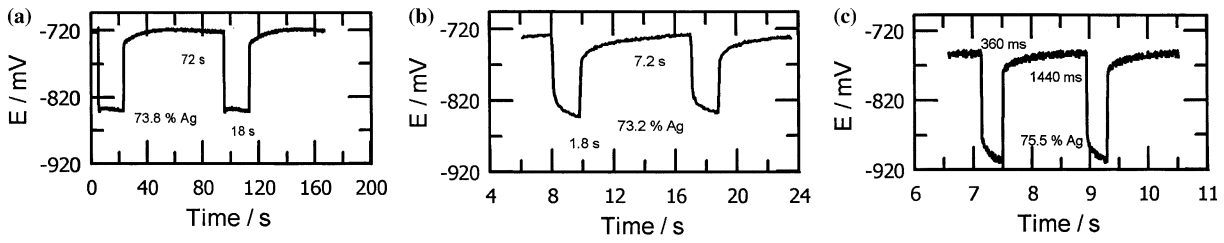

Fig. 3. Changes in the cathodic potential during pulsed electrodeposition C_{Ag} = 8 g dm^{-3}, C_{Bi} = 18 g dm^{-3}; J_1:J_2 = 0.8:0.2 A dm^{-2}; t_1:t_2 = 1:4 (a) 160 sublayer, t_1:t_2 = 18:72 s, 26.2 wt.% Bi, 0.115 μm sublayer (b) 1600 sublayer, t_1:t_2 = 1.8:7.2 s, 26.8 wt.% Bi, 0.012 μm sublayer (c) 8000 sublayer, t_1:t_2 = 360:1440 ms, 25 wt.% Bi, 0.002 μm sublayer.

registered. As the number of sublayers increases, the overall compressive stress also increases and, similarly to the case of equal sublayer thickness (J_1:J_2 = 0.8:0.2 A dm^{-2} and t_1:t_2 = 1:4), it approaches the internal stress of multilayer coatings electrodeposited at 0.8 A dm^{-2}.

The type of the initial or final sublayer of the system does not substantially affect the sign of the overall internal stress of multilayer coatings. Figure 9 shows two different cases when the multilayer coating starts either with a silver-rich (0.2 A dm^{-2}) or a bismuth-rich (0.8 A dm^{-2}) sublayer. In both cases the overall internal stress of the coating is negative.

A comparison between the internal stress alterations at three different ratios of sublayer thickness is shown in the case of 4 (Figure 10) and 400 sublayers (Figure 11). In both cases the stress transition from positive to negative with increase in the effect of the bismuth-richer sublayer is again noticed. Figure 11 also shows that if suitable current densities (J_1:J_2 = 0.8:0.2 A dm^{-2}) and thickness of the two sublayers are correctly selected (t_1:t_2 = 1:4, 400 sublayers) it is possible to deposit strain-free coatings. Probably similar multilayer coatings can combine the properties of the individual sublayers and at relatively high total percentage content of bismuth in the alloy (approx. 30 wt.%) to remain stress-free.

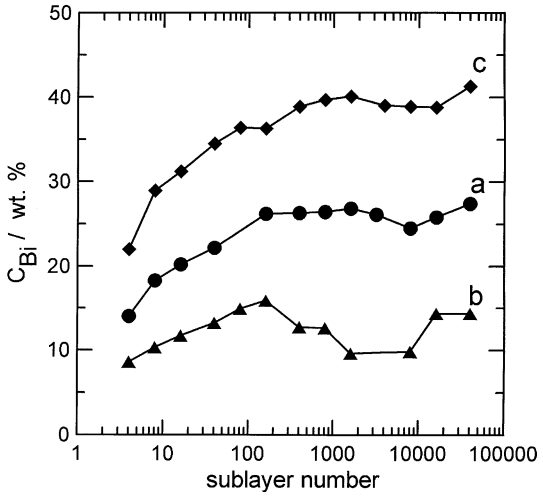

Fig. 4. Bismuth content with increasing sublayer number C_{Ag} = 8 g dm^{-3}, C_{Bi} = 18 g dm^{-3} (a) J_1:J_2 = 0.8:0.2 A dm^{-2}, t_1:t_2 = 1:4 (b) J_1:J_2 = 0.8:0.2 A dm^{-2}, t_1:t_2 = 1:9 (c) J_1:J_2 = 0.8:0.2 A dm^{-2}, t_1:t_2 = 2:3.

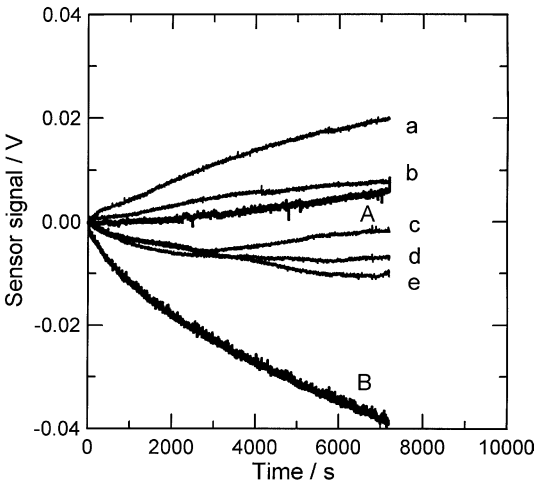

Fig. 6. Change of the sensor signal with time C_{Ag} = 8 g dm^{-3}, C_{Bi} = 18 g dm^{-3}; J_1:J_2 = 0.8:0.2 A dm^{-2}; t_1:t_2 = 1:9 (A) monolayer, 0.2 A dm^{-2}, 0.7 wt.% Bi, 12.5 μm (B) monolayer, 0.8 A dm^{-2}, 50 wt.% Bi, 26.3 μm (a) 400 sublayer, 12.7 wt.% Bi, 16.3 μm (b) 800 sublayer, 12.6 wt.% Bi, 16.3 μm (c) 1600 sublayer, 9.6 wt.% Bi, 16.2 μm (d) 8000 sublayer, 9.8 wt.% Bi, 16.3 μm (e) 16000 sublayer, 14.3 wt.% Bi, 17.6 μm.

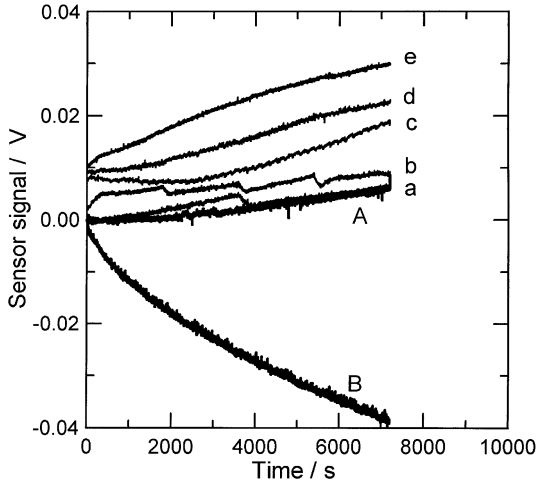

Fig. 5. Change of the sensor signal with time C_{Ag} = 8 g dm^{-3}, C_{Bi} = 18 g dm^{-3}; J_1:J_2 = 0.8:0.2 A dm^{-2}; t_1:t_2 = 1:9 (A) monolayer, 0.2 A dm^{-2}, 0.7 wt.% Bi, 12.5 μm (B) monolayer, 0.8 A dm^{-2}, 50 wt.% Bi, 26.3 μm (a) 4 sublayer, 8.6 wt.% Bi, 17.6 μm (b) 8 sublayer, 10.3 wt.% Bi, 16.6 μm (c) 80 sublayer, 14.9 wt.% Bi, 17.1 μm, (U–U_o) + 0.008 V (d) 160 sublayer, 17.9 wt.% Bi, 17.3 μm, (U–U_o) + 0.009 V.

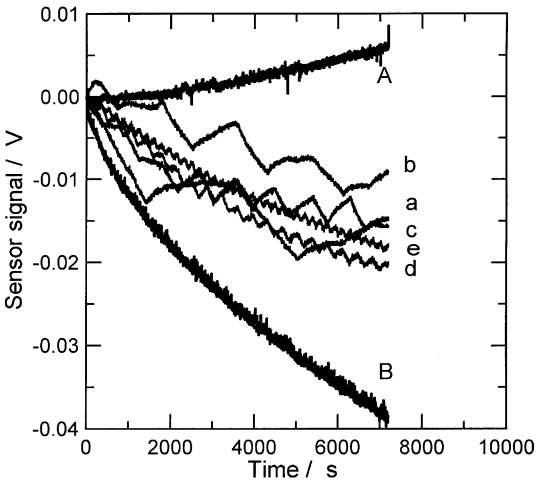

Fig. 7. Change of the sensor signal with time C_{Ag} = 8 g dm^{-3}, C_{Bi} = 18 g dm^{-3}; J_1:J_2 = 0.8:0.2 A dm^{-2}; t_1:t_2 = 2:3 (A) monolayer, 0.2 A dm^{-2}, 0.7 wt.% Bi, 12.5 μm (B) monolayer, 0.8 A dm^{-2}, 50 wt.% Bi, 26.3 μm (a) 4 sublayer, 22 wt.% Bi, 20.6 μm (b) 8 sublayer, 28.3 wt.% Bi, 22.7 μm (c) 16 sublayer, 31.2 wt.% Bi, 21.9 μm (d) 40 sublayer, 34.9 wt.% Bi, 23.1 μm (e) 160 sublayer, 36.4 wt.% Bi, 22.7 μm.

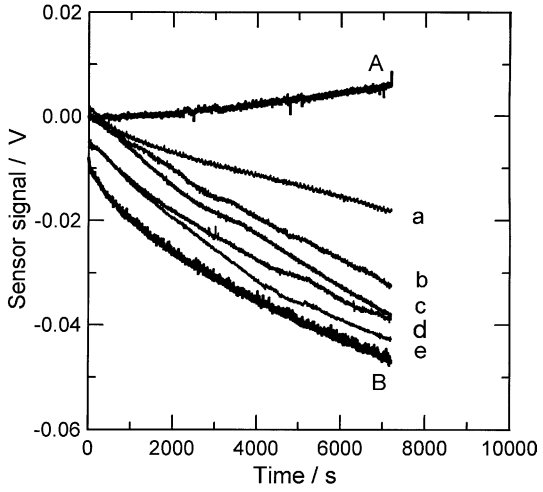

Fig. 8. Change of the sensor signal with time $C_{Ag}=8$ g dm^{-3}, $C_{Bi}=18$ g dm^{-3}; $J_1{:}J_2=0.8{:}0.2$ A dm^{-2}; $t_1{:}t_2=2{:}3$ (A) monolayer, 0.2 A dm^{-2}, 0.7 wt.% Bi, 12.5 μm (B) monolayer, 0.8 A dm^{-2}, 50 wt.% Bi, 26.3 μm, $(U-U_o)$ – 0.008 V (a) 160 sublayer, 36.3 wt.% Bi, 22.7 μm (b) 400 sublayer, 32.8 wt.% Bi, 25.0 μm (c) 1600 sublayer, 40.1 wt.% Bi, 24.3 μm (d) 4000 sublayer, 39.0 wt.% Bi, 23.9 μm, $(U-U_o)$ – 0.005 V (e) 16000 sublayer, 38.8 wt.% Bi, 23.9 μm, $(U-U_o)$ – 0.006 V.

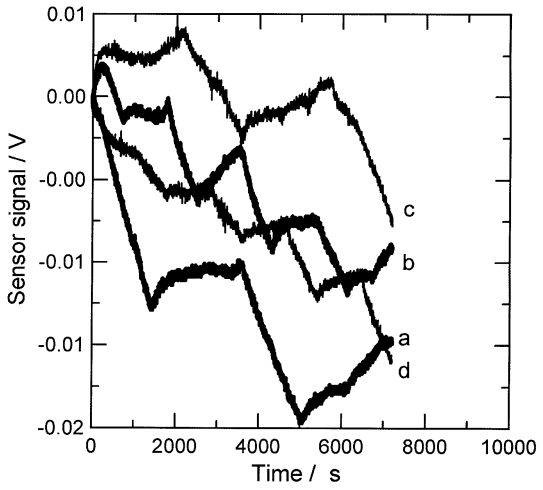

Fig. 9. Change of the sensor signal with time $C_{Ag}=8$ g dm^{-3}, $C_{Bi}=18$ g dm^{-3} $J_1{:}J_2=0.8{:}0.2$ A dm^{-2}; $t_1{:}t_2=2{:}3$ (a) 4 sublayer, 22.0 wt.% Bi, 20.6 μm (b) 8 sublayer, 28.9 wt.% Bi, 22.1 μm $J_1{:}J_2=0.2{:}0.8$ A dm^{-2}; $t_1{:}t_2=3{:}2$ (c) 4 sublayer, 45.9 wt.% Bi, 27.6 μm (d) 8 sublayer, 41.0 wt.% Bi, 25.0 μm.

The cross–sections of multilayer coatings show a discontinuous structure (Figure 12). In contrast to Ag–Sb systems [14], the Ag–Bi alloy does not form homogeneous sublayers. A similar behaviour may be related to the fact that bismuth forms island films onto the silver substrate (Figures 13 and 14). The islands represent polycrystalline formations and have a relatively fine–grained crystalline basis and a coarser crystalline upper part. Probably bismuth is deposited considerably easier on its own substrate than onto silver and thus enhances the discontinuous growth of the sublayers. Sometimes dendritic multilayer growth is observed (Figure 15).

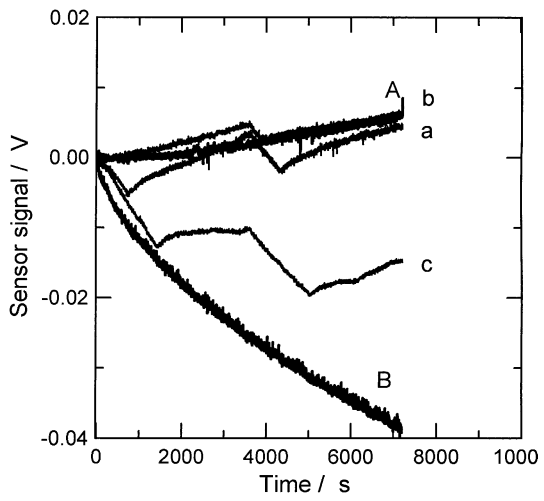

Fig. 10. Change of the sensor signal with time; 4 sublayer $C_{Ag}=8$ g dm^{-3}, $C_{Bi}=18$ g dm^{-3} (a) $J_1{:}J_2=0.8{:}0.2$ A dm^{-2}, $t_1{:}t_2=1{:}4$, 18.1 μm (b) $J_1{:}J_2=0.8{:}0.2$ A dm^{-2}, $t_1{:}t_2=1{:}9$, 17.6 μm (c) $J_1{:}J_2=0.8{:}0.2$ A dm^{-2}, $t_1{:}t_2=2{:}3$, 24.4 μm.

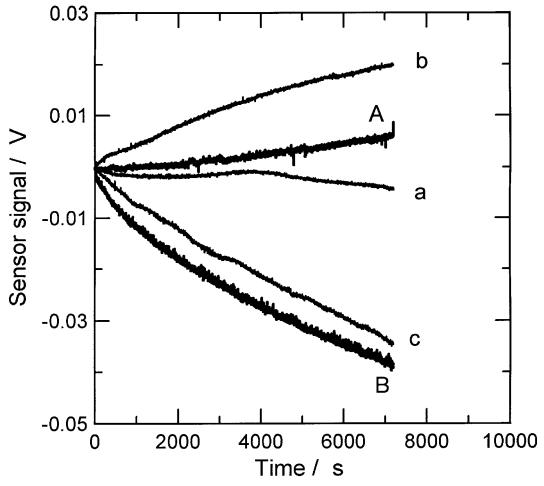

Fig. 11. Change of the sensor signal with time; 400 sublayer $C_{Ag}=8$ g dm^{-3}, $C_{Bi}=18$ g dm^{-3} (a) $J_1{:}J_2=0.8{:}0.2$ A dm^{-2}, $t_1{:}t_2=1{:}4$, 20.4 μm (b) $J_1{:}J_2=0.8{:}0.2$ A dm^{-2}, $t_1{:}t_2=1{:}9$, 16.3 μm (c) $J_1{:}J_2=0.8{:}0.2$ A dm^{-2}, $t_1{:}t_2=2{:}3$, 27.6 μm.

In such cases the overall internal stress of the coating cannot be determined correctly due to the undefined thickness of the coating, but the changes in the sensor signal could provide information about their sign.

4. Conclusions

- In multilayer coatings the positive internal stress of the silver-rich sublayers is combined with the negative stress of the bismuth-rich sublayers. The stress in the multilayer coating depends on the overall bismuth content in the deposit resulting from the ratio of the current densities, as well as of the pulse durations applied.
- The internal stress of the cyclically modulated Ag–Bi multilayer also depends on the sublayer number. At

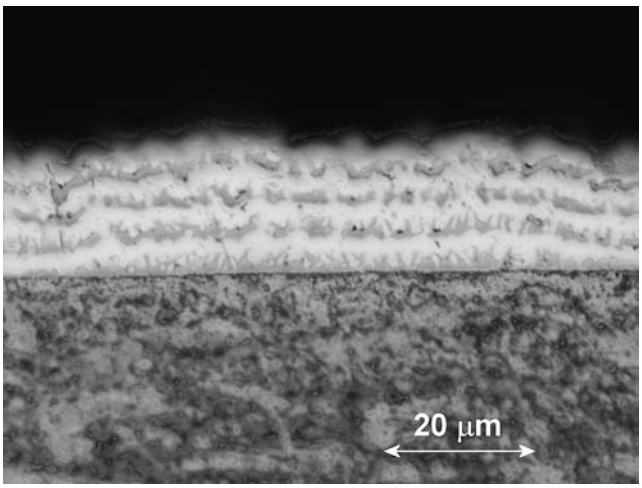

Fig. 12. Cross section of a multilayer alloy coating $C_{Ag} = 8$ g dm^{-3}, $C_{Bi} = 18$ g dm^{-3}; $J_1{:}J_2 = 0.8{:}0.2$ A dm^{-2}; $t_1{:}t_2 = 1{:}4$ 8 sublayer, 20.2 wt.% Bi, 18.9 μm.

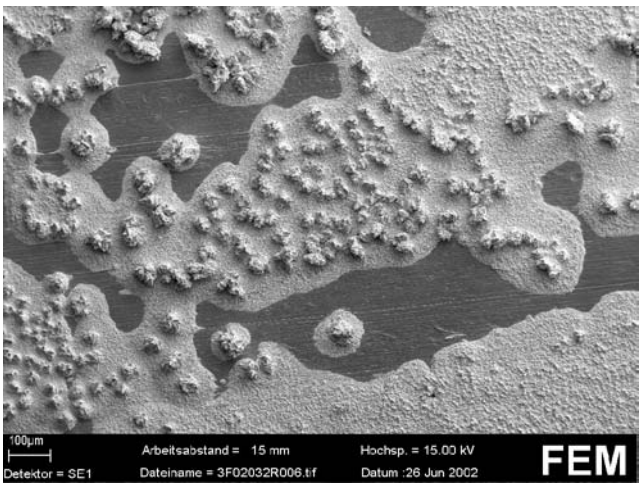

Fig. 13. Island layers of bismuth-rich phase on the silver substrate J = 0.8 A dm^{-2}.

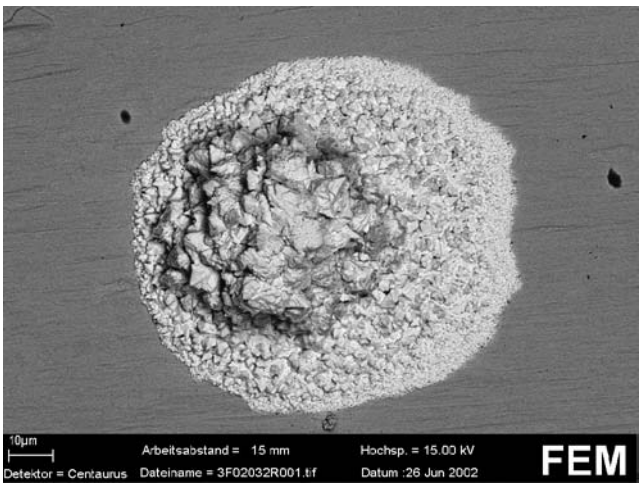

Fig. 14. Bismuth-rich island of the layer of Figure 13.

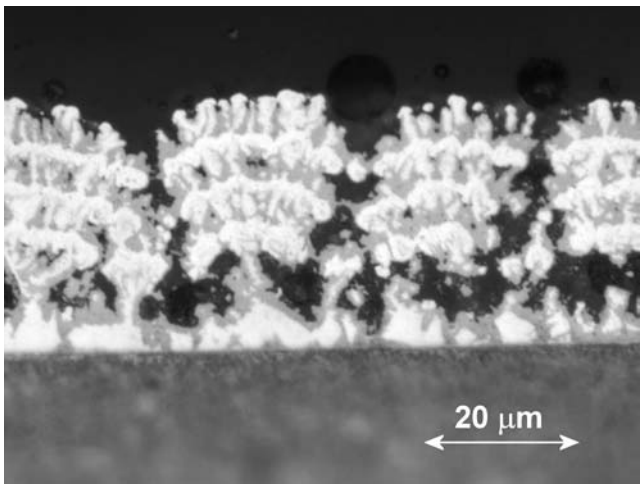

Fig. 15. Cross section of a dendritic multilayer coating $C_{Ag} = 8$ g dm^{-3}, $C_{Bi} = 18$ g dm^{-3}; $J_1{:}J_2 = 0.2{:}0.8$ A dm^{-2}; $t_1{:}t_2 = 3{:}2$ 8 sublayer, 41.4 wt.% Bi, 25 μm.

appropriate deposition conditions stress-free multilayer coatings can be obtained.

- The bismuth-rich sublayers are discontinuous due to the peculiarities of the bismuth deposition on silver substrate.

Acknowledgements

The present studies are part of a joint research project between the Institute of Physical Chemistry of the Bulgarian Academy of Sciences, Sofia and Forschungsinstitut für Edelmetalle und Metallchemie, Schwäbisch Gmünd. The authors express their gratitude to Deutsche Forschungsgemeinschaft for the financial support of project 436 BUL 113/97/0–3.

References

1. P.M. Vjacheslavov, S.J. Grilihes, G.K. Burkat and E.G. Kruglova, *Galvanotehnika blagorodnih i redkih metallov*, Mashinostroenie, Leningrad, 1 ed. (1970), 5 (in Russian).
2. I. Kristev and M. Nikolova, *J. Appl. Electrochem.* **16** (1986) 867.
3. I. Krastev, N. Petkova and A. Zielonka, *J. Appl. Electrochem.* **32** (2002) 811.
4. P.M. Vjacheslavov, *Novie elektrokhimicheskie pokritija*, Lenizdat, Leningrad, 1 ed. (1972), 220 (in Russian).
5. USA Patent 590 412 (1943).
6. T. Valkova and I. Krastev, *Trans. Inst. Metal Finish.* **80** (2002) 13.
7. T. Valkova and I. Krastev, *Trans. Inst. Metal Finish.* **80** (2002) 16.
8. T. Valkova and I. Krastev, *Trans. Inst. Metal Finish.* **80** (2002) 21.
9. I. Krastev, T. Valkova and A. Zielonka, *J. Appl. Electrochem.* **33** (12) (2003) 1199.
10. M. Hansen and K. Anderko, *Constitution of binary alloys* 1 (McGraw Hill Book Co. Inc, New York, 1958), p. 23.
11. E. Raub and A. Engel, *Zeitschrift für Metallkunde* **41** (1950) 485.
12. I. Krastev, T. Valkova and A. Zielonka, *J. Appl. Electrochem.* **34** (1) (2004) 79.
13. M. Stalzer, *Metalloberfläche* **18** (1964) 263.
14. I. Krastev and A. Zielonka, *J. Appl. Electrochem.* **32** (2002) 1141.
15. M. Monev, I. Krastev and A. Zielonka, *J. Phys.: Condens. Mat.* **49** (1999) 10033.